

PHOTOLUMINESCENCE OF ULTRADISPERSE ALUMINA CERAMICS UNDER VUV EXCITATION

V. S. Kortov, V. A. Pustovarov, T. V. Spiridonova,*
and S. V. Zvonarev

UDC 535.331.34;535.37;539.23

Photoluminescence (PL) spectra of anion-defective alumina single crystals and ultradisperse ceramics were measured under excitation in the vacuum ultraviolet (VUV) region. Emission bands in the experimental PL spectrum were identified using a developed technique to reconstruct spectra of luminescent dielectrics. A correspondence was found between the calculated and experimental PL spectra of α -Al₂O₃ single crystal. The PL spectrum of ultradisperse anion-defective alumina ceramic was calculated taking into account luminescence centers created by intrinsic and impurity defects. Bands in the experimental spectrum were identified based on it.

Keywords: alumina, anion-defective ceramics, photoluminescence, synchrotron radiation.

Introduction. Alumina with oxygen vacancies in the anion sublattice is a luminophore with unique dosimetric properties. Highly sensitive detectors TLD-500 are fabricated from single crystals of anion-defective corundum (α -Al₂O₃) for monitoring ionizing radiation in the low-dose range [1, 2]. They are widely used for personal dosimetry and environmental radiation monitoring. Powders of anion-defective α -Al₂O₃ with particle sizes in the nanometer range (20–60 nm) possess enhanced radiation resistance and can be used as high-dose radiation detectors [3]. Obviously, ceramics synthesized from nanopowders are most promising for practical applications of high-dose radiation detectors. Luminescent ceramics with high stability and high mechanical strength are suitable for mass production of detectors of given sizes.

Moreover, high-temperature (1200–1500°C) synthesis of α -Al₂O₃ ceramics from nanopowders is associated with an increase of nanoparticle size that reaches several hundreds of nanometers depending on the temperature and synthesis time [4]. Such ceramics represent a new class of luminophores consisting of ultradisperse particles, the size of which is 1.5–2 orders of magnitude less than industrial powder luminophores with crystal sizes 20–40 μ m. It can be assumed that ceramics synthesized from nanopowders will inherit some properties characteristic of nanopowders, especially those that depend on surface features and increased defectiveness at particle boundaries. It has already been confirmed experimentally that anion-defective α -Al₂O₃ ceramics can be used to measure high-dose radiation [5]. Also, the properties of luminophores with particle sizes intermediate between nanometer and micrometer ranges are little studied.

Herein photoluminescence (PL) spectra of anion-defective alumina ceramics were studied experimentally. Emission centers were identified based on computer calculations that enabled emission bands of impurity centers and centers created by intrinsic defects to be reconstructed.

Experimental. Nanopowders of alumina were prepared beforehand by electric explosion of aluminum wire in order to synthesize the luminescent ceramics [6]. Subsequent sedimentation enabled batches of weakly aggregated powders with relatively homogeneous particle sizes in the range 20–70 nm to be obtained. Chemical analysis of the starting alumina nanopowders was performed on a PDS-2 spectrometer by atomic emission with arc excitation and gave the following results (impurity, mass%): Cr, $1.8 \cdot 10^{-4}$; Ti, $3 \cdot 10^{-4}$; Mg, $2 \cdot 10^{-3}$; Fe, $1 \cdot 10^{-2}$. Thus, the starting nanopowders contained several impurities that luminesce in the Al₂O₃ matrix, of which Mg and Fe had the highest concentrations. X-ray powder patterns obtained using a D8 Discover diffractometer, CuK α -radiation, and a graphite monochromator established the presence in the powders of metastable alumina phases γ (65%) and δ (35%). The powders were subjected to pulsed magnetic compaction [7] at ~ 2 GPa pressure and 450°C. This enabled blanks for experimental samples to be prepared as pellets 10–15 mm in diameter and up

*To whom correspondence should be addressed.

to 1 mm thick. The obtained samples were sintered at 1550°C for 30 min in a vacuum furnace (10^{-4} Torr) in order to prepare the ceramics. Heat treatment at this temperature was needed for complete conversion of the unstable γ - and δ -phases into the stable alumina α -phase. The ceramics had to be synthesized in vacuo in order to create in them oxygen vacancies that acted as electron traps. A scanning electron microscope (SEM, Zeiss Sigma VP) with a Schottky cathode was used to analyze the sizes and shapes of the particles on the ceramic surface.

Single crystals of anion-defective α -Al₂O₃ grown from raw material of nominal purity that was purified by zone melting were studied for comparison. The content of each of the aforementioned luminescent impurities in it was $<1 \cdot 10^{-4}$ mass% except for Cr ($1.3 \cdot 10^{-4}$ mass%). Single crystals were grown by the Stepanov method from the melt in the presence of carbon, which provided reducing conditions [8]. According to optical absorption data, the concentration of F-centers created by oxygen vacancies with two captured electrons was $\sim 1.3 \cdot 10^{17}$ cm⁻³. The studied single crystals were transparent disks 1-mm thick and 5-mm in diameter.

Considering the broad band gap of Al₂O₃ (9.4 eV) and the need for high excitation density, experimental PL spectra of anion-defective ceramics were recorded with excitation by pulsed synchrotron radiation in the VUV region ($E_{\text{ex}} = 10.8$ eV) at the Superlumi station (Hamburg, HASYLAB Laboratory, Channel I, DESY synchrotron) [9]. An ARC SpectraPro-300i monochromator (0.3 m) and Hamamatsu R6358P photomultiplier tube (PMT) were used for the recording. Experimental PL spectra of single-crystalline samples of anion-defective Al₂O₃ were measured on a McPherson VUVAS 1000+ vacuum spectrometer with steady-state excitation in the far UV region ($E_{\text{ex}} = 7.7$ eV). Measurements were made at room temperature. The radiation source was a deuterium lamp (150 W). A McPherson 2035 monochromator and R928 PMT were used for the recording.

Results and Discussion. Figure 1 shows an SEM photomicrograph of the surface of the synthesized ceramic. It can be seen that the surface was dominated by agglomerates of various shapes, the sizes of which varied in different parts of the surface in the range 500–1000 nm. It is also noteworthy that the ceramics were opaque. Therefore, a thin surface layer consisting of agglomerates and particles incorporated in them luminesced. The luminescing centers were concentrated primarily at the boundaries.

Figure 2 shows the PL spectrum of ultradisperse Al₂O₃ ceramic excited by synchrotron radiation. Only two bands could be identified in the first stage. The first weak luminescence peak *A* at 208 nm could be explained by emission of excitons bound to defects [4]. The second peak *B* at 320 nm corresponded to the PL band of the known F⁺-center created in α -Al₂O₃ by an oxygen vacancy that captured one electron [10]. The excited state of the F⁺-center was split into three sublevels under the influence of the crystal field. Optical absorption bands at 4.8, 5.4, and 6.3 eV corresponded to transitions from the ground state into the excited state [10]. All states of the F⁺-center corresponding to these absorption bands were excited by irradiation of the sample with synchrotron radiation of energy 10.8 eV. Emission of the F⁺-center at 325 nm that was due to singlet–singlet transitions $1B \rightarrow 1A$ was observed.

Other components of the PL spectrum of the ceramic samples were identified using the developed technique for reconstruction of emission spectra of intrinsic and impurity luminescence centers. The technique was based on computer calculation of a superposition of Gaussians with known positions of spectral band maxima and their half-widths in addition to band broadening for nano-sized samples. It was assumed that electron–hole pairs were generated during excitation by photons of energy $E_{\text{exc}} > E_{\text{g}}$ and that recombination processes that formed a Gaussian emission band occurred. The recombination energy could also excite intracenter transitions.

Experimental results for the positions of band maxima and emission line half-widths were used in the present work as initial parameters for the calculations. The following equation was proposed for describing the band intensities $I(h\nu)$ in the PL spectra:

$$I(h\nu) = \sum_{i=1}^n \left[\frac{1}{U_i} \left(\frac{\pi}{2} \right)^{1/2} \right] G_i \exp \left(- \left(2 [E_{\text{exc}} - E_{\text{mi}}] / U_i \right)^2 \right), \quad (1)$$

where U_i is the half-width of the i -th emission line; G_i , the generation rate of electron–hole pairs that was calculated for each center taking into account the absorption coefficient; E_{mi} , the energy position of the i -th peak; and n , the number of luminescence bands in the PL spectrum.

The change of line width ΔU was considered in calculating PL spectra of samples with ultradisperse and nano-sized structures. This could be described by the following formula [11]:

$$\Delta U = h\nu_{\text{f}}R + \varphi(R)/R^2, \quad (2)$$

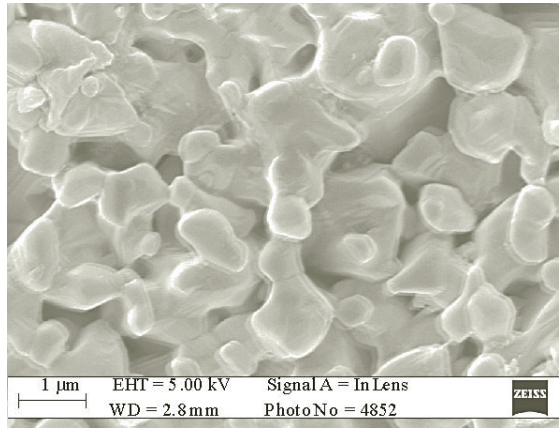


Fig. 1. SEM image of ultradisperse α -Al₂O₃ ceramic surface.

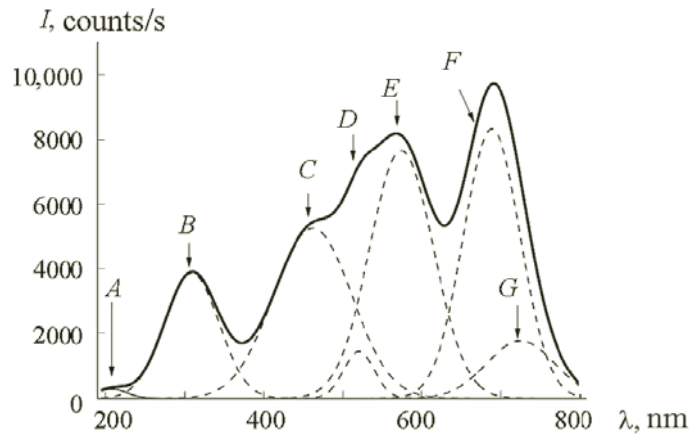


Fig. 2. Photoluminescence spectrum of ultradisperse α -Al₂O₃ ceramic with excitation by synchrotron radiation ($E_{\text{exc}} = 10.8$ eV, $T = 7.6$ K).

where v_f is the velocity of free charge carriers (cm/s); h , Planck's constant; and $\varphi(R)$, a function depending on the particle size R . The technique is discussed in more detail in the literature [12].

PL spectra of anion-defective single-crystalline α -Al₂O₃ samples with steady-state excitation by a beam of VUV photons were calculated and measured in order to check the adequacy of the developed technique (Fig. 3). It was found that two principal bands were present in the experimental spectrum of nominally pure single-crystalline Al₂O₃ and corresponded to F-centers and centers created by Cr³⁺ ions. Excitation of the F-center caused PL with a maximum at 410 nm (triplet-singlet transition ${}^3P \rightarrow {}^1S_0$). The luminescence band of F⁺-centers (325 nm) was not recorded (curve 2) because the PMT in the spectrometer had spectral sensitivity in the range 400–1600 nm. The following reactions causing luminescence occurred for F- and F⁺-centers in α -Al₂O₃: $e^- + F^+ \rightarrow F^* \rightarrow F + h\nu$ (410 nm) and $h^+ + F \rightarrow F^{+*} \rightarrow F^+ + h\nu$ (325 nm) [10]. The PL spectrum of impurity Cr³⁺-centers contained a narrow R-line with a maximum at 693 nm that corresponded to the transition ${}^2E \rightarrow {}^4A_2$ and also satellites associated with phonon generation [13]. The agreement of the calculated and experimental PL spectra of the studied single-crystalline α -Al₂O₃ samples could be considered satisfactory despite the fact that the calculation did not enable phonon tails to be found in the emission spectrum of Cr³⁺.

It is noteworthy on switching to the identification of bands in the experimental PL spectrum of the anion-defective Al₂O₃ ceramic with the ultradisperse structure that bands of aggregate F₂-centers (two vacancies with four captured electrons) could be expected in addition to bands of the aforementioned F- and F⁺-centers that were created by single oxygen vacancies. It is well known that such centers and their charged analogs (F₂⁺ and F₂²⁺-centers) arise in α -Al₂O₃ crystals upon

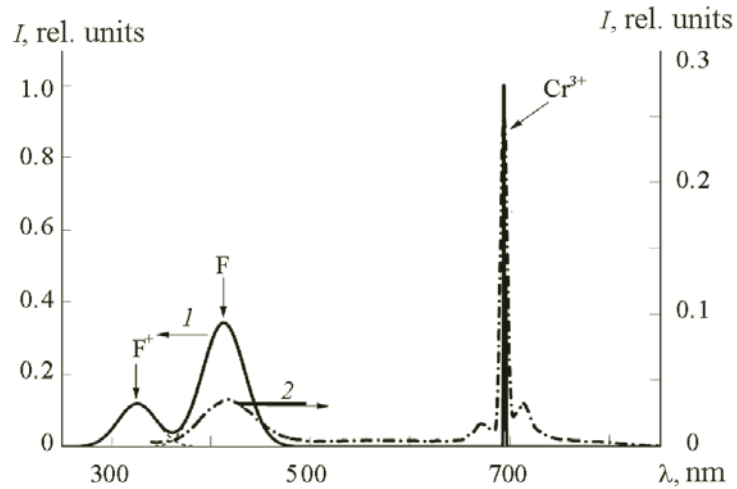


Fig. 3. Calculated (1) and experimental (2) photoluminescence spectra of single-crystalline α - Al_2O_3 with VUV excitation ($E_{\text{exc}} = 7.7$ eV, $T = 300$ K).

TABLE 1. Principal Photoluminescence Parameters of Emission Centers in Anion-Defective α - Al_2O_3

Center	λ_m , nm	U , nm	Reference
F	415.0	30.000	[10, 15]
F^+	325.0	27.000	[10, 15]
F_2	500.0	18.750	[15, 16]
F_2^{2+} (2Mg)	520.0	9.750	[14, 16]
F_2^+ (2Mg)	750.0	9.000	[14, 16]
Ti^{4+}	570.0 440.0	45.000	[17, 18]
Ti^{3+}	725.0	18.000	[17, 18]
Cr^{3+}	692.9 694.3	0.375	[4, 13]
Fe^{3+}	567.0 674.5 670.9	31.500 3.750	[19, 20]

high-temperature treatment in vacuo [14]. According to the chemical analysis, PL centers created by impurity Mg, Fe, Cr, and Ti ions should be present in the studied ceramic. Table 1 presents parameters known from the literature for bands presumably present in PL spectra of the studied samples of anion-defective Al_2O_3 ceramic. These parameters were used as initial input for reconstructing the spectra. The concentration of intrinsic F-centers varied in the range 10^{17} – 10^{18} cm^{-3} , which agreed with the literature [10, 14–16]. The concentration of impurity centers was calculated from results of the chemical analysis and varied in the range 10^{16} – 10^{18} cm^{-3} . The greatest values were obtained for F^+ -centers and also for impurity Mg^{2+} - and Fe^{3+} -centers.

The PL spectrum of ultradisperse α - Al_2O_3 ceramic was calculated for excitation parameters corresponding to the experimental ones, i.e., synchrotron radiation beam with photon energy $E_{\text{exc}} = 10.8$ eV, pulse length $t_p = 1$ ns, and sample

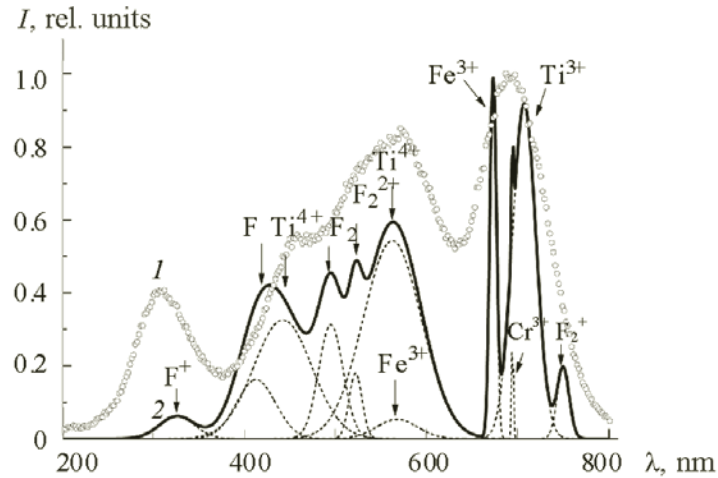


Fig. 4. Experimental (1) and calculated (2) photoluminescence spectra of ultradisperse α - Al_2O_3 ceramic with excitation by 10.8-eV photons.

temperature 7.6 K (Fig. 4). The spectrum contained two broad peaks in the visible region that could be associated with the presence of green emission bands of aggregate F_2^- and F_2^{2+} (2Mg)-centers in addition to the bands of F- and F^+ -centers noted above. It is well known that the aggregate center F_2^{2+} (2Mg) represents two oxygen vacancies, the charge of which is compensated by two Mg ions [14]. The reactions for creation and emission of this center are: $2V_a + 2\text{Mg}^{2+} \rightarrow \text{F}_2^{2+}$ (2Mg) and $2h^+ + \text{F}_2 \rightarrow \text{F}_2^{2+}$ (2Mg) $^* \rightarrow \text{F}_2^{2+}$ (2Mg) + $h\nu$ (520 nm), where V_a is the oxygen vacancy. The emission reaction of the F_2^- -center is: $2e^- + \text{F}_2^{2+}$ (2Mg) $\rightarrow \text{F}_2^* \rightarrow \text{F}_2 + h\nu$ (500 nm). A group of bands of a Ti^{4+} impurity center with maxima at 440 and 570 nm could also be identified [17]. Blue (non-locally compensated Ti^{4+} ions) and green (locally compensated Ti^{4+} ions) emission components of an impurity Ti^{4+} center appeared as a result of the reaction: $h^+ + \text{Ti}^{3+} \rightarrow \text{Ti}^{4+*} \rightarrow \text{Ti}^{4+} + h\nu$ (440 and 570 nm) [18]. Fe^{3+} ions, luminescence of which corresponded to a $d-d$ radiative transition for electrons of a d^5 -shell (${}^4T_1 \rightarrow {}^6A_1$), contributed to a broad PL band at 570 nm [19].

PL bands in the red spectral region with a maximum at 750 nm could be caused by emission of an aggregate F_2^+ (2Mg)-center (oxygen divacancy, the charge of which is compensated by two Mg ions that capture three electrons). Also, Cr^{3+} , Ti^{3+} , and Fe^{3+} ions were also responsible for the red emission. The contribution to the red band of F_2^+ (2Mg) centers was also noteworthy. These appeared as a result of electron capture at an F_2^{2+} (2Mg)-center. Emission of this center arose from the reaction: F_2^{2+} (2Mg) + $e^- \rightarrow [\text{F}_2^+ \text{ (2Mg)}]^* \rightarrow \text{F}_2^+ \text{ (2Mg)} + h\nu$ (750 nm).

Another two emission lines at 670 and 674 nm were observed in spectra of ultradisperse samples of Al_2O_3 containing Fe impurity. According to the literature [20], these bands arose from the transition ${}^4T_1 \rightarrow {}^6A_1$. The PL spectrum of impurity Cr^{3+} -centers contained a narrow R -line with a maximum at 690 nm, like for the single crystal. Two components of the R -line (R_1 at 694.3 nm and R_2 at 692.9 nm) could be recorded at low temperatures. The doublet could not be resolved in spectra of the studied samples. The following transformation causing PL occurred for Cr ions: $h^+ + \text{Cr}^{2+} \rightarrow \text{Cr}^{3+*} \rightarrow \text{Cr}^{3+} + h\nu$ (693 nm). Emission of Cr^{3+} -centers was due to the transition ${}^2E \rightarrow {}^4A_2$ [13]. The emission band of the Ti^{3+} -center had a maximum at 720 nm. The absorption spectrum of Ti^{3+} -centers contained a broad line at 2.5 eV that corresponded to the transition ${}^2T_2 \rightarrow {}^2E$ [21]. Emission arose from the reaction: $e^- + \text{Ti}^{4+} \rightarrow \text{Ti}^{3+*} \rightarrow \text{Ti}^{3+} + h\nu$ (720 nm) [18].

Based on the analysis, a conclusion could be drawn about the nature of the bands in the experimental PL spectrum of ultradisperse anion-defective Al_2O_3 ceramic (Fig. 2). Peak A was due to excitons associated with defects; peak B, F^+ ; peak C, superposition of F and Ti^{4+} -centers; peak D, superposition of F_2^- and F_2^{2+} -centers; peak E, superposition of Ti^{4+} - and Fe^{3+} -centers; peak F, superposition of Fe^{3+} -, Cr^{3+} -, and Ti^{3+} -centers; peak G, F_2^+ . For convenience, the experimental PL spectrum is shown in Fig. 4 together with the calculated one.

Conclusions. PL spectra of anion-defective single-crystalline α - Al_2O_3 were obtained upon excitation in the VUV region. A technique for reconstructing the PL spectra was used to calculate emission bands of the single crystal. The agreement of the experimental and calculated spectra indicated that the used reconstruction technique was adequate for the PL spectra. PL spectra of anion-defective Al_2O_3 ceramic with an ultradisperse structure were measured upon excitation by pulsed

synchrotron radiation in the VUV region. The emission spectrum of the studied ceramic was calculated taking into account luminescence of centers created by oxygen vacancies and impurity defects in order to identify the observed PL bands. The calculated PL spectrum had a shape close to the experimental one. This enabled bands to be identified in the experimental spectrum. An analysis of the results showed that a feature of the PL of anion-defective α -Al₂O₃ ceramic PL upon VUV excitation was a large contribution of aggregate F-centers to the emission spectrum.

Acknowledgments. The work was supported financially by a grant of the RF President for State Support of Young Russian Scientists (Contract No. 14.125.13.4696-MK), a grant of the OPTEK Carl Zeiss for support of young scientists of leading higher educational institutions and scientific research centers 2012/2013 (Contract No. 20/2013 of May 21, 2013), and a grant for young scientists of First President of Russia B. N. Yeltsin Ural Federal University under the auspices of its development program (Contract No. 1.2.2.3/63).

REFERENCES

1. S. W. S. McKeever, M. Moscovitch, and P. D. Townsend, *Thermoluminescence Dosimetry Materials: Properties and Uses*, Nucl. Tech. Pub., Ashford (1995).
2. V. Kortov, *Radiat. Meas.*, **42**, 576–581 (2007).
3. N. Salah, Z. H. Khan, and S. S. Habib, *Nucl. Instrum. Methods Phys. Res., Sect. B*, **269**, 401–404 (2011).
4. V. A. Pustovarov, V. S. Kortov, S. V. Zvonarev, and A. I. Medvedev, *J. Lumin.*, **132**, 2868–2873 (2012).
5. V. Kortov and Yu. Ustyantsev, in: *Proc. 7th Int. Workshop on Ionizing Radiation Measurement*, Japan (2011), pp. 281–294.
6. Yu. A. Kotov, *J. Nanopart. Res.*, **5**, 539–550 (2003).
7. V. Ivanov, S. Paranin, and A. Nozdrin, *Key Eng. Mater.*, **132–136**, 400–403 (1997).
8. M. S. Akselrod, V. S. Kortov, and E. A. Gorelova, *Radiat. Prot. Dosim.*, **54**, 353–356 (1994).
9. G. Zimmerer, *Radiat. Meas.*, **42**, 859–864 (2007).
10. B. D. Evans, *J. Nucl. Mater.*, **219**, 202–223 (1995).
11. I. P. Suzdalev, *Nanotechnology: Physicochemistry of Nanoclusters, Nanostructures, and Nanomaterials*, KomKniga, Moscow (2006).
12. V. S. Kortov, T. V. Spiridonova, and S. V. Zvonarev, *Poverkhnost*, **10**, 107–112 (2013).
13. A. B. Kulinkin, S. P. Feofilov, and R. I. Zakharchenya, *Fiz. Tverd. Tela*, **42**, 835–838 (2000).
14. M. G. Rodriguez, G. Denis, M. S. Akselrod, T. H. Underwood, and E. G. Yukihara, *Radiat. Meas.*, **46**, 1469–1473 (2011).
15. A. I. Surdo, V. A. Pustovarov, V. S. Kortov, A. S. Kishka, and E. I. Zinin, *Nucl. Instrum. Methods Phys. Res., Sect. A*, **543**, 234–238 (2005).
16. E. A. Kotomin, A. Stashans, L. N. Kantorovich, A. I. Lifshitz, A. I. Popov, and I. A. Tale, *Phys. Rev. B: Condens. Matter Mater. Phys.*, **51**, No. 14, 8770–8779 (1995).
17. B. D. Evans and M. Stapelbroek, *Phys. Rev. B: Condens. Matter Mater. Phys.*, **18**, No. 12, 7089–7098 (1978).
18. G. Molnar, M. Benabdesselam, J. Borossay, D. Lapraz, P. Iacconi, V. S. Kortov, and A. I. Surdo, *Radiat. Meas.*, **33**, 663–667 (2001).
19. C. Mo, L. Zhang, X. Yao, and X. Fan, *J. Appl. Phys.*, **76**, 5453–5456 (1994).
20. T. Monteiro, C. Boemare, M. J. Soares, E. Alves, C. Marques, C. McHargue, L. C. Ononye, and L. F. Allard, *Nucl. Instrum. Methods Phys. Res., Sect. B*, **191**, 638–643 (2002).
21. L. E. Bausa, I. Vergara, F. Jaque, and J. Garcia Sole, *J. Phys.: Condens. Matter*, **2**, 9919–9925 (1990).